REPRESENTING POLYMER MODIFIED BITUMEN IMAGES USING TEXTURAL FEATURES

Ş. GÜMÜŞTEKİN[1], A. TOPAL[2], B. SENGOZ[2], S. MARKANDAY[3], G. POLACCO[3]
[1] *Izmir Institute of Technology, Department of Electrical & Electronics Engineering, 35430, Urla, Izmir, TURKEY*
[2] *Dokuz Eylul University, Faculty of Engineering, Civil Engineering Department, Tinaztepe Campus, 35160, Buca, Izmir, TURKEY*
[3] *Universita ` di Pisa, Dipartimento di Ingegneria Chimica, Chimica Industriale e Scienza dei Materiali (DICCISM), Universita ` di Pisa, Largo LucioLazzarino 2, Pisa 56122, ITALY*

ABSTRACT

This study aims to analyze the textural features extracted from microscopic images of organoclay nanocomposite, styrene butadiene styrene (SBS); ethylene vinyl acetate (EVA), and ethylene butyl acrylate (EBA) polymer modified bitumens (PMB) with polymer composition variation. Fluorescence microscopy was employed to capture the microscopic images from thin films of PMB samples at different magnification scales (40x, 100x, 400x). Gabor filters were utilized to extract the textural features of bitumen images. The dimensionality of the feature space was reduced from 72 to 2 by using different techniques to enable visualization of distinct classes. The results indicated that, texture analysis makes it possible to accurately identify samples that belong to a particular class (i.e. a particular content and/or a particular polymer type).

Keywords: Polymer modified bitumen, Nanocomposite, Texture analysis, Gabor filters, Microscopic image

1 INTRODUCTION

In recent years, major emphasis has been placed on improving the performance of bituminous mixtures in order to construct long lasting road pavements and to minimize deterioration such as permanent deformation, low temperature and fatigue cracking and moisture susceptibility. In order to improve bitumen characteristics, specific performance enhancers have been investigated. These include additive modification, polymer modification and chemical reaction modification [1].

The polymers that are used for bitumen modification can be divided into two main groups, named as elastomers and plastomers [2]. Within the elastomeric group, styrene butadiene styrene (SBS) block copolymers and within the plastomeric group, ethylene vinyl acetate (EVA) and ethylene butyl acrylate (EBA) have shown the greatest potential when blended with base bitumen [3].

Due to the invention of nano clays in 1990 by Toyota research [4,5] and their success in improvement of Nylon-6 [6] with an addition of small quantity of nano clay, the materials world witnessed an innovative material called polymer nanocomposite. Within few years, thermoplastic elastomer based nanocomposite was patented [7]. Later, several studies (e.g. [8, 9]) reported the use of nano clay in bitumen. Desirable characteristics of polymer modified bitumen (PMB) include greater elastic recovery, viscosity, cohesive strength, ductility and a higher softening point [10, 11].

Fluorescent microscopy has been used for the determination of the quality of the dispersion of PMB for many years. The captured images have been used for a subjective judgment of the quality of the PMB comparison with other images of PMBs. This method does not give much information to the PMB producers and additional tests must be performed to determine the quality of PMBs. The visual investigation of the images is concerned with the textures that are due to different dispersion characteristics which can be related to chemical and physical properties. In order to eliminate the need for subjective evaluations, texture analysis methods can be utilized to achieve automatic visual inspection.

Extraction of textural features from captured images and using these features for various classification problems have been widely studied [12]. These studies target many different applications that utilize image understanding to solve specific problems. Recently, the use of textural properties of PMB images was introduced in [13].

In this paper, a further analysis of textural properties is carried out with utilization of reduced feature spaces which allow visual inspection. This allows us to observe the degree of class separation ambiguity. It also makes it possible to select suitable image capturing parameters (e.g. magnification) for a specific classification problem. Besides using the data which was used in [13] to illustrate the reduced feature spaces, organoclay nanocomposite, plastomeric and elastomeric and PMB images were used in a similar texture analysis.

2 PREPERATION AND FLUORESCENCE MICROSCOPY IMAGE CAPTURE OF PMB SAMPLES

The base bitumen was procured from Aliaga/Izmir Oil Terminal of the Turkish Petroleum Refinery Corporation. The bitumen was 50/70 penetration grade conventional asphalt from vacuum distillation, with ring and ball softening point (RB) = 49°C and penetration = 63 dmm. The type of nano clay utilized for nano composite preparation was Cloisite 20A® (subsequently referred to as CL) from Southern Clay Products, USA. CL is an organoclay prepared from a sodium montmorillonite having a cation exchange capacity of 0.926 meq·g^{-1} by treatment with 0.95 meq.g^{-1} of $Me_2(HT)_2NH_4Cl$ (dimethyldihydrogenated-tallow ammonium chloride). From the base bitumen, polymer modified bitumens with 6% EVA (by weight) were prepared. These are referred to as PMA6. The EVA-clay nanocomposites, with weight ratio always set to 60:40, were prepared by the two different blending methods. In ternary systems B/EVA/clay the first method used physical mixing (PM) in which the polymer and clay were added separately to the base bitumen during the modification procedure. The second method used EVA/CL nanocomposites prepared by melt blending (MB) in the modification process of the base bitumen. The EVA/CL blends were prepared by melt compounding in a Brabender Plasticorder static mixer, preheated to 190°C. The organoclay was added to the molten polymer before increasing the rotor speed to 60rpm. After the extraction from the mixer the samples were cooled naturally in the atmosphere.The complete list of the studied system nanoclay is given in Table 1.

The EBA (Elvaloy®3427), EVA (Evatene® 2805, Elvaloy®4170), and SBS (Kraton® D1101, Soltene® 6302) modified bitumen samples were prepared by means of a high and a low shear laboratory type mixer rotating at 1100 rpm and 125 rpm, respectively. In preparation, the base bitumen was heated to fluid condition (180–185 ^{o}C), and poured into a 2000 ml spherical flask. The EBA, EVA, and SBS polymers were then added slowly to the base bitumen.

The EBA and EVA concentrations in the base bitumen were chosen as 2 %–6 % and 3 %–7 % respectively according to the manufacturers. The concentrations of SBS in the base bitumen were also chosen as 2 % to 6 % by weight. The utilization of this content was based on past research made by Isacsson and Lu [2]. They concluded that a significant improvement in the properties of base bitumen was observed when the SBS content was increased from 2 % to 6 % by weight.

The temperature was kept constant at 185 ^{o}C, and the mixing process continued for 2 hours. The uniformity of dispersion of EBA, EVA and SBS in the base bitumen was confirmed by passing the mixture through an ASTM 100# sieve. After completion, the samples were removed from the flask and divided into small containers, covered with aluminum foil and stored for testing.

Table 1: Composition and preparation of the nanocomposites

System	EVA (wt %)	CL (wt %)	Prep. Method
PMA6 (R6)	6	-	-
6/20A/PM (R6N)	6	4	PM
6/20A/MB (R6P)	6	4	MB

In describing the microstructure interacting between bitumen and polymer, the term "morphology" is often used [14]. Fluorescence microscopy is used to investigate the morphology of the EBA, EVA, and SBS PMBs by determining the state of dispersion of the polymer within the base bitumen as well as to characterize the nature of the continuous and discontinuous phase. Fluorescence microscopy is a valuable tool for studying the phase morphology of PMB, as it allows the observation of the homogeneity and the structure in the raw state [15].
Fluorescence microscopy is based on the principle that polymers swell due to the absorption of some of the constituents of the base bitumen. Due to the fluorescence effect of the aromatic compounds of bitumen, the bitumen rich phase appears dark or black, whereas the polymer rich phase appears light [16] (e.g. Fig. 1).
Samples of each PMB were prepared (for imaging purposes) by using a standard sample preparation method that involves a heating and homogenizing procedure a sample cooling regime as well as a surface preparation procedure over thin films of the samples [17]. PMB samples were examined at room temperature under a Leica DM EP microscope with fluorescent light (generated from a high pressure Xenon lamp) at magnification levels of 400×, 100×, and 40×. Images were then taken by a 7.2 Mp Leica DFC 320 color camera fitted in line with the optic axis of the microscope by means of an attachment to the trinocular observation head. The camera digitizes the image and stores the data as an image file in the hard drive of the workstation.

3 EXTRACTION OF TEXTURAL FEATURES FROM RESPONSES OF GABOR FILTERS

Textural features of images are usually extracted by applying a series of mathematical transformations and measurements that quantify image deviations in different scales and orientations. One of the most common techniques for extracting textural features is texture analysis using Gabor filters [18]. Filter responses corresponding to different frequency scales and orientations can be used as textural features that characterize physical properties of image data. Gabor filters are widely used in many different applications of texture analysis such as content based image retrieval [19–22], remote sensing [23, 24], fault detection [25, 26], biometric identification [27–33], medical image analysis [34, 35], object recognition [36, 37], optical text processing [38–40], etc.
Gabor filters can be implemented using an oriented and scaled set of Gaussian filters and they can be designed to cover the spatial frequency space uniformly as illustrated in Fig. 1. Details on the design of Gabor filters can be found in [13,18]. The main idea here is to design filters with unique spatial frequency characteristics. The response of each filter on input images corresponds to signal content in a specific frequency band and a specific spatial orientation.

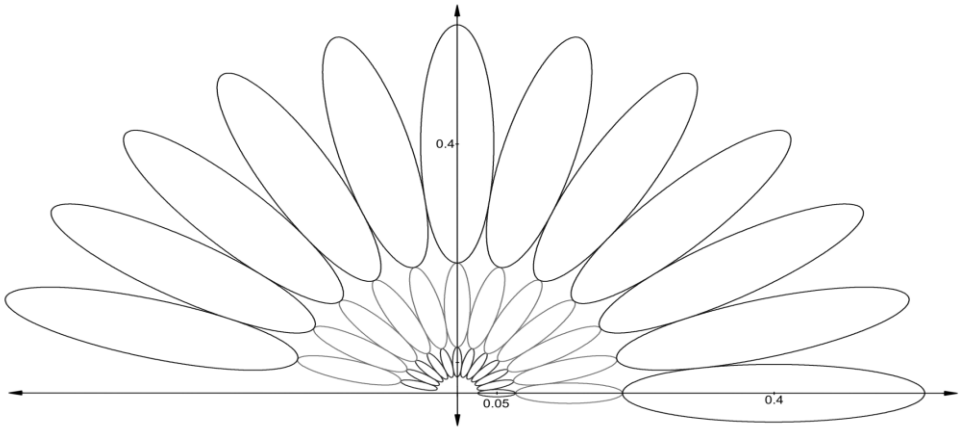

Figure 1: Isocontours of Gabor filter responses at half peak values in spatial frequency space for 12 orientations and 3 scales.

Gabor filters can be applied to an N×M image $I(x, y)$ by:

$$I_{mn}(x, y) = \sum_{p} \sum_{q} I(x - p, y - q) G^{*}_{mn}(x, y) \tag{6}$$

where "*" is used for the complex conjugate. This Gabor filter corresponds to scale *m* and orientation *n*. This is illustrated in Fig. 2 where Gabor filters are applied for 3 scales and 12 orientations on the sample image. Magnitudes of the complex images are displayed.

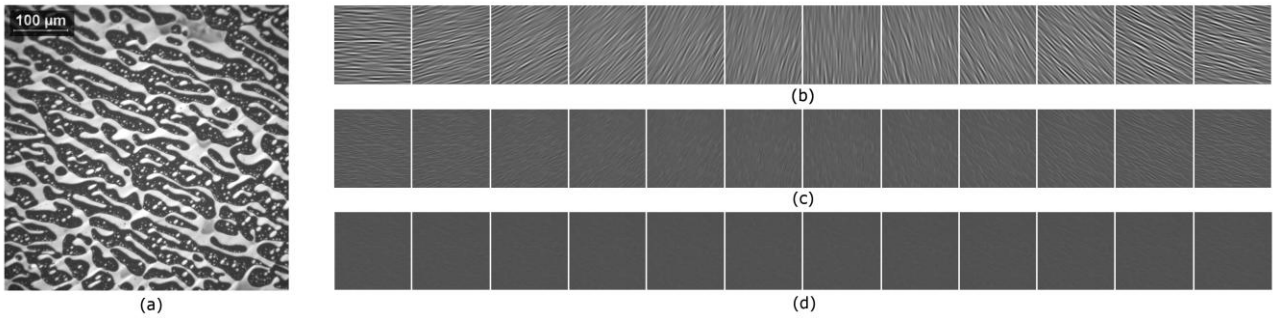

Figure 2: (a) Sample texture: 100× magnified bitumen with 6 % Elvaloy® 3427, (b) Magnitudes of Gabor filter responses for 12 different orientations (columns) and 3 different scales (rows).

Average values and deviation values of S×K (i.e. number of scales × number of orientations) images are used as the textural features [13, 36]:

$$\mu_{mn} = \frac{\sum_x \sum_y |G_{mn}(x,y)|}{MN} \quad , \quad \sigma_{mn} = \sqrt{\frac{\sum_x \sum_y (|G_{mn}(x,y)| - \mu_{mn})^2}{MN}} \tag{7}$$

A feature vector can be formed by cascading mean and deviation values for all *m* and *n*:

$$\boldsymbol{F} = \{\mu_{00}, \sigma_{00}, \mu_{10}, \sigma_{10}, ..., \mu_{(S-1)0}, \sigma_{(S-1)0}, ..., \mu_{(S-1)(K-1)}, \sigma_{(S-1)(K-1)}\} \tag{8}$$

The distance between two feature vectors $\boldsymbol{F}^{(i)}$ and $\boldsymbol{F}^{(j)}$ extracted from two images can be defined as:

$$d(i,j) = \sqrt{\sum_m \sum_n \left(\frac{\mu_{mn}^{(i)} - \mu_{mn}^{(j)}}{\sigma_{\mu(m,n)}}\right)^2 + \left(\frac{\sigma_{mn}^{(i)} - \sigma_{mn}^{(j)}}{\sigma_{\sigma(m,n)}}\right)^2} \quad , \quad m = 0,1,...,S-1 \quad n = 0,1,...,K-1 \tag{9}$$

The distance metric used here is the Euclidian distance between the terms which are normalized by standard deviation. The order of feature values in the feature vectors is directly related to the orientation of the textures. As depicted in Fig. 2, it can be seen that the dominant texture orientation causes the filter responses to have a higher degree of variations for the Gabor filters steered in that particular direction. Texture analysis applications should be able to identify textures correctly even if they are rotated in an arbitrary direction. Several approaches have been proposed to make the texture analysis rotation invariant [41–46]. These methods generally depend on mapping feature points to a different space with rotation invariance properties (by Fourier Transform, etc.) or reorganizing feature vectors by rotational shift operations. In this study, different approaches are adopted for rotational invariance of Gabor features. One of these approaches is based on finding the most dominant orientation and reorganizing the feature values by a rotational shift such that the peak value is placed at the leftmost position [41]. Another approach is based on calculating the distance between two feature vectors by circularly shifting one of the vectors and using the shift position that gives the minimum distance between the two vectors.

After different types of bitumen (i.e. base and modified by organoclay, EBA, EVA, and SBS) images were captured using a microscope-mounted digital camera, three different approaches (named A, B and C) were tested on the images to see how well Gabor features represent image textures. The A, B and C methods can be summarized as:

Method A: Direct use of Gabor features (with no effort to satisfy rotation invariance).

Method B: The peak value corresponding to the orientation with highest energy is computed and the feature vector is circularly shifted until the peak value is placed at the leftmost position.

Method C: One of the feature vectors were circularly shifted for all possible cases and its distance to the second feature is calculated for each of these cases and the minimum distance value is recorded.

4 K-NEAREST NEIGHBOR (K-NN) CLASSIFICATION

The K-NN classification [47] is one of the classical techniques that allow classification of samples in a feature space merely based on their distances to training samples. For each query sample, the class that contains the most of the nearest *k* samples is assigned as the class for the query sample. The choice of *k* is limited by 1 and the number of samples in each training class. A choice of small *k* may lead to complicated decision boundaries that may be negatively affected by outlier samples. A large *k* introduces smooth decision regions at the expense of increased computational burden and lost local selectivity. In this paper performance results are computed for five values of *k* (from 1 to 5) and

the average values are reported. The K-NN classifier is tested on the Gabor features of modified bitumen using the leave-one-out (LOO) cross validation technique.
For each query sample with a known class, the rest of the samples are used as the training set. The rate of query samples correctly classified by K-NN is recorded as the success rate for the query class.

5 REDUCTION OF DIMENSIONALITY BY TRANSFORMING FEATURE SPACE

Real data observed from raw measurements usually inhibits high dimensionality. Dimensionality reduction is needed to represent the data with minimal complexity that corresponds to the intrinsic dimensionality. When raw measurement data, which may include highly correlated and/or unrelated term, is used, misleading interpretations (due to a phenomenon known as "curse of dimensionality) may result as intrinsic dimensionality is over exceeded. Besides, dimensionality reduction is useful for purposes of compression and visualization of data. In this paper, a reduction of dimensionality is done not to estimate an optimal feature space that complies with intrinsic dimensionality, but to visualize textural features extracted from images.
In a review, several linear and nonlinear techniques for reduction of dimensionality is presented [48]. As discussed in this review, no clear advantage can be claimed for each of these different techniques. The ability of these techniques to represent data is highly dependent on the form of the data. Therefore, multiple space reduction techniques can be used together to robustly represent data in the reduced dimensionality.
Technical details about these methods are out of the scope of this paper. Dimensionality reduction techniques are used in two different data sets. In Fig.3, the Gaussian Process Latent Variable Model (GPLVM) is used on the PMB data of [13] for illustration of class separation for the classes comprising PMB of different mixture rates using images of different magnifications. The results corresponding to other dimensionality reduction techniques are omitted here due to lack of space. Fig.4 shows the case where labeled classes correspond to different types of modification.
Nine different dimensionality reduction techniques are used together on another set of data extracted from images of organoclay nanocomposite PMBs (Fig.6).

6 RESULTS AND DISCUSSION

A human observer can easily distinguish structural characteristics of modified bitumen images. In order to perform the operation on a computer automatically, the key features of the images that are common in the same class of images, but are not typically shared in different classes should be identified. Textural features are shown to be useful in the process of discrimination between different classes.
Two different datasets are used in the experiments. First, Gabor features are extracted from the data used in [13] which contains twelve PMB images of different polymer type and content rate. These features correspond to responses of filters as illustrated in Fig.2. The 72 dimensional feature space is reduced to 2D using Gaussian Process Latent Variable Model (GPLVM). Fig.3 and Fig.4 exhibit the distribution of the feature points in the reduced feature space. Each column in these figures corresponds to different magnification factors (40x, 100x, and 400x) used during image capturing. The clustering nature of feature points belonging to the same class is clearly visible in most of the figures. The results are consistent with the classification results given in [13]. When compared to interpretation of the numerical classification results, the graphical interpretation given here seems to be easier and more effective.
The second dataset used was a set of organoclay nanocomposite PMB images. Samples randomly selected from these images are presented in Fig.5. 80 images for each of R6, R6N, R6P classes were used in a k-NN classification test. For each sample, rest of the dataset is treated as a training set and the class that contains the closest k samples is accepted as the sample class. This is repeated for k values from 1 to 5 and the average classification score is used for the final classification of sample. As shown in Table 2, a high percentage of sample images are correctly classified by k-NN. This test indicates that the classes studied here (i.e. R6, R6N, R6P) are highly separable.

Table 2: Classification results for organoclay nanocomposite modified bitumen classes.

	Method 1	**Method 2**	**Method 3**
R6	99.75%	100%	99.75%
R6N	100%	100%	98.75%
R6P	100%	100%	100%
Average:	99.92%	100%	99.50%

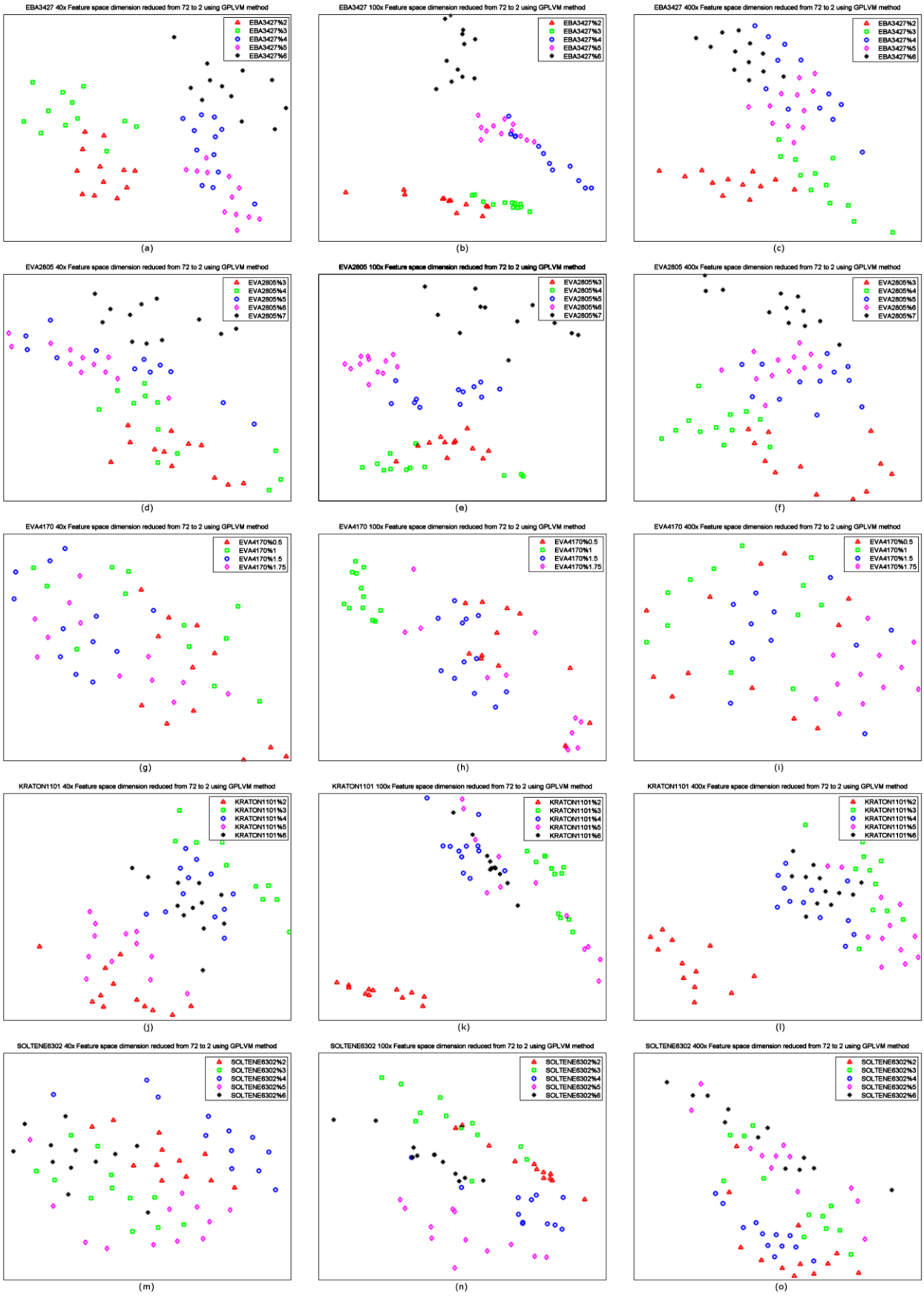

Figure 3: Plots of feature space with dimensionality reduced from 72 to 2 using Gaussian Process Latent Variable Model (GPLVM) on features extracted from (40x,100x,400x) images of bitumen with (a,b,c) Elvaloy® 3427, (d,e,f) Evatene® 2805, (g,h,i) Elvaloy® 4170, (j,k,l) Kraton® D1101, (m,n,o) Soltene® 6302. Classes denoted as different geometric shapes and colors, correspond to different percentages of polymers.

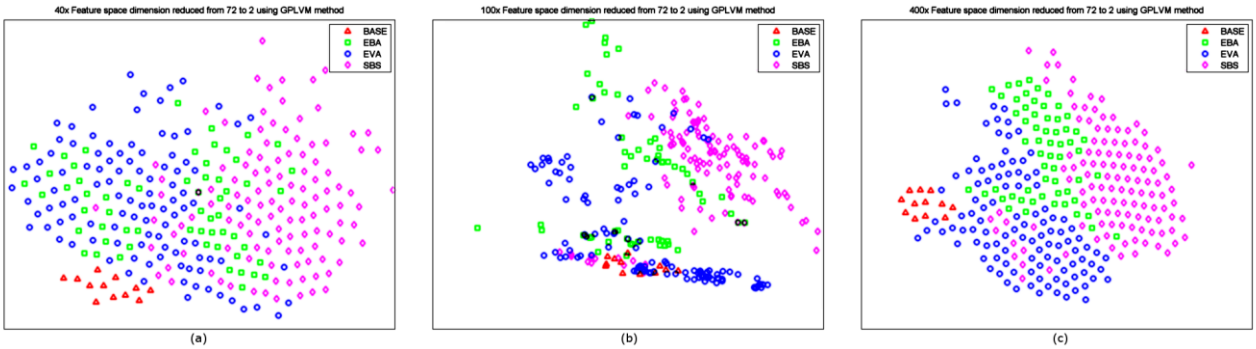

Figure 4: Plots of feature space with dimensionality reduced from 72 to 2 using GPLVM on features extracted from (40x,100x,400x) images of combined data set. Classes correspond to different types of polymers. Each type of class may include samples with mixtures of different percentages.

To verify the classification results graphically, nine different techniques are used to reduce the dimensionality of the feature space to 2D. As shown in Fig.6, the feature points are clearly separable with a small ambiguity even though the dimensionality is not necessarily selected to be greater than the intrinsic dimensionality of the data. It can also be observed that different data reduction techniques can isolate different classes more clearly. So, using multiple techniques for dimensionality reduction is helpful for observing specific classes besides providing more reliable data.

7 CONCLUSIONS

This paper addresses the problem of characterizing microscopic modified bitumen images using textural features. These features are extracted from images which are constructed by applying Gabor filters on bitumen images. Gabor filters are a set of Gaussian filters which partition frequency space. The response of each filter provides a description of the signal content at a specific frequency band and a spatial orientation. Each filter response is represented by mean and deviation values (Eq. 7). Mean and deviation values for all filter responses are combined to form a feature vector. In our case the size of this feature vector is 72 (i.e. 3 frequency scales x 12 orientations x 2 feature values). In the analysis, the initial step is the computation of features for each bitumen image. Each image is represented by a feature vector. In [13] it was shown that, textural features extracted from images of polymer modified bitumen (PMB) inhibit structural characteristics of samples that make it possible to discriminate between different classes such as different types of modification, different percentage of polymer content, etc.

In this paper, Gabor features that belong to several classes of PMB are transformed into 2D space by dimensionality reduction from 72 to 2 to enable visualization of data. This makes it possible to verify the discriminative properties of features by visual inspection. The textural features extracted from the data set studied in [13] are mapped to 2D space using Gaussian Process Latent Variable Model (GPLVM). A visual examination of clusters in reduced feature space verifies the classification results given in [13]. The degree of ambiguity in class separation is clearly visible in the reduced feature space. This makes it possible to choose parameters of image capture (e.g. magnification) that are most convenient for a specific classification task.

Another data set comprising plastomeric, elastomeric and organoclay nanocomposite PMB images was also used in a similar texture analysis. It is shown that the classes in this data set are completely separable using classification based on k-NN method and Gabor features. Textural features of this data set are mapped to 2D space using 9 different methods. All of these 9 representations display clusters of feature points with small or no overlap between classes. Using different dimensionality reduction methods together seems to be helpful since the success of each method is strongly dependent on different properties of the data.

It is shown that image based characterization of bitumen samples can be effectively done by discriminating between different classes in the space of textural features. Textural analysis of PMB images may lead to many different applications such as quality control inspection, identification, etc.

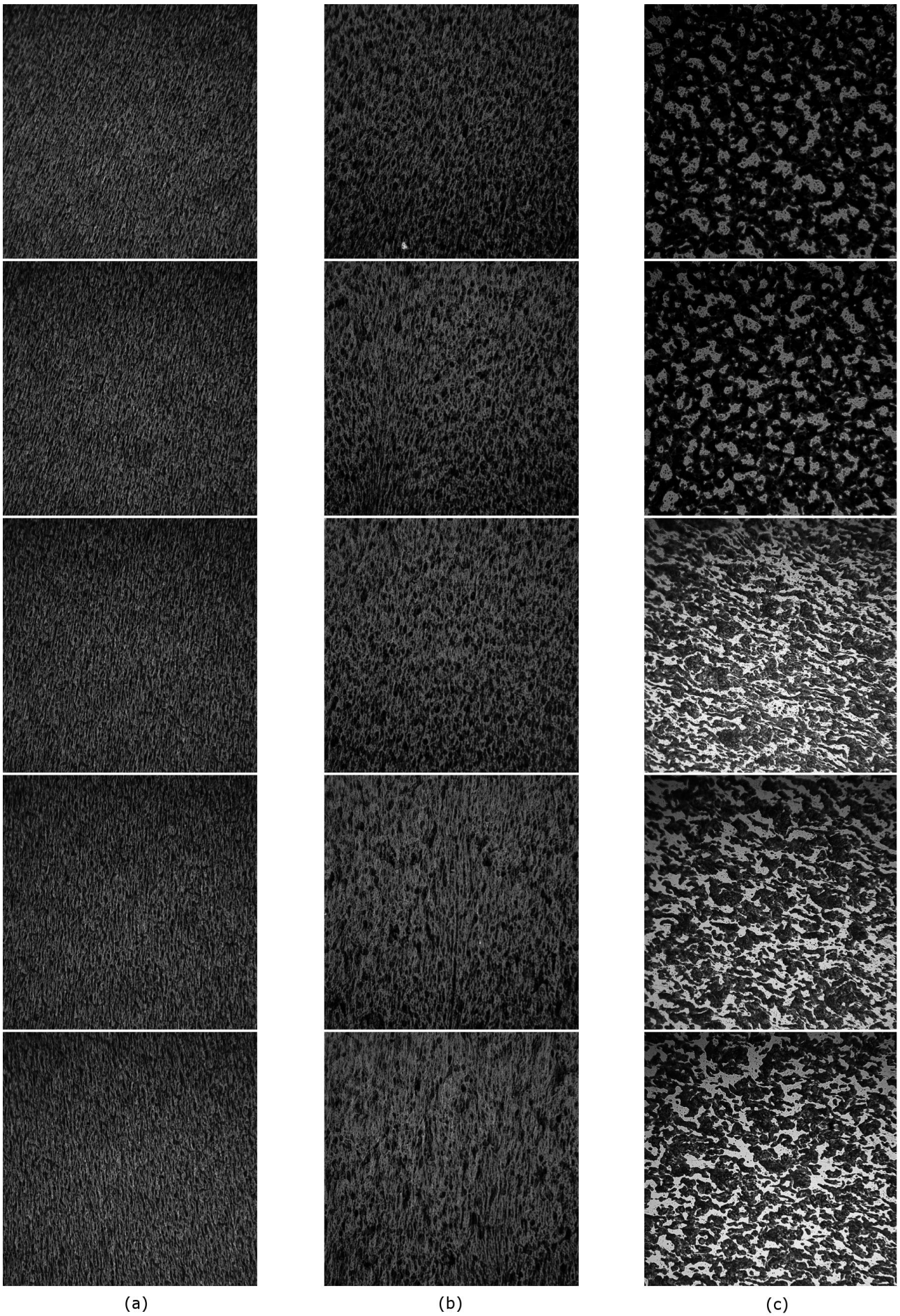

Figure 5: 5 sample images arbitrarily selected from a set of 80 images of type (a) R6, (b) R6N, (c) R6P.

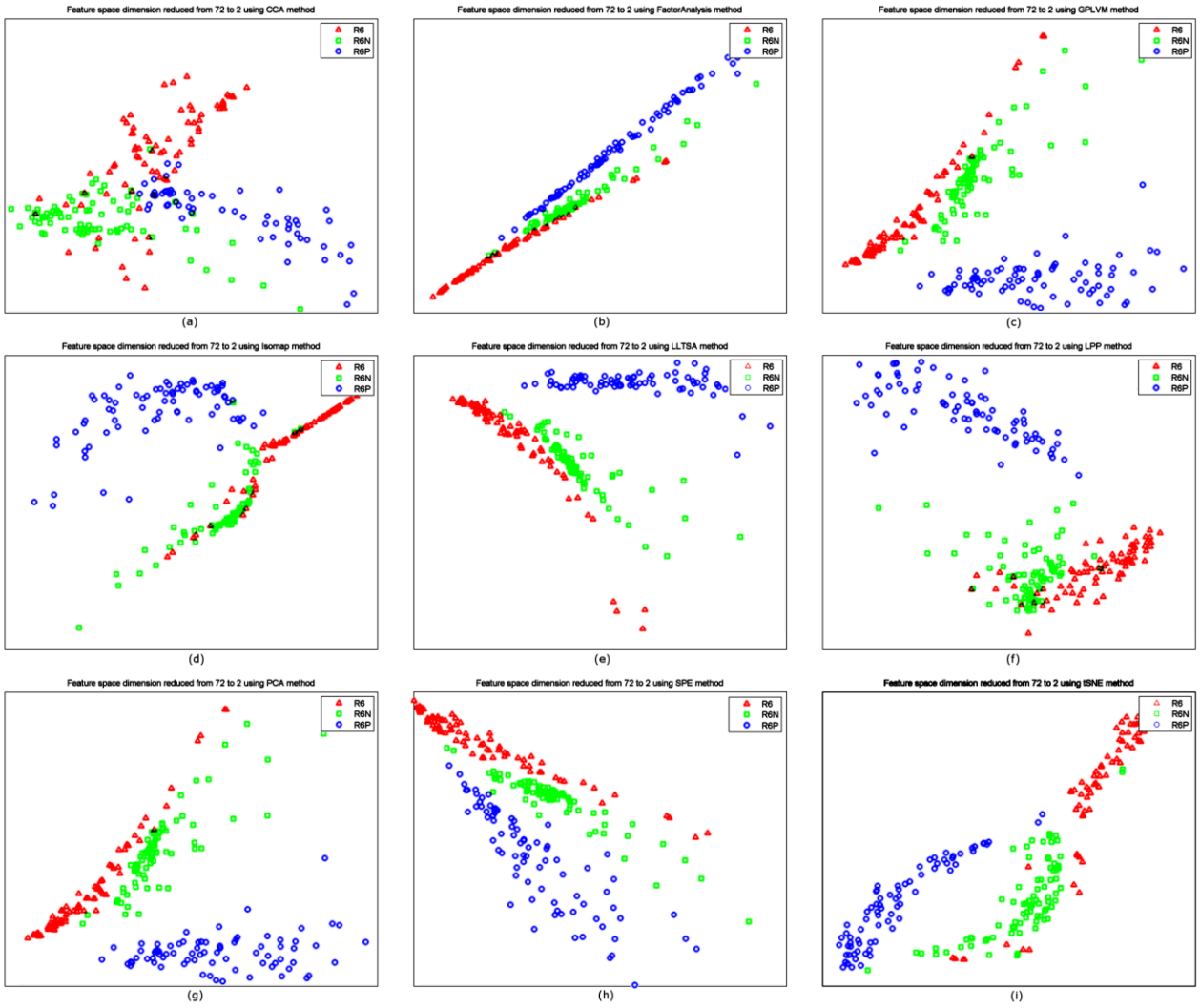

Figure 6: Plots of feature space with dimensionality reduced from 72 to 2 using (a) Conformal Component Analysis, (b) Factor Analysis (c) Gaussian Process Latent Variable Model , (d) Isomap, (e) Linear Local Tangent Space Alignment, (f) Linearity Preserving Projection, (g) Principle Component Analysis, (h) Stochastic Proximity Embedding, (i) T-Distributed Stochastic Neighbor Embedding

REFERENCES

[1] Characterization of Bitumens Modified with SBS, EVA and EBA Polymers, Isacsson U., and Lu X., J. Materials Science, No.34, pp.3737 – 3745, 1999.

[2] Rheological Evaluation of Ethylene Vinyl Acetate Polymer Modified Bitumens, Airey, G., J. Constr. Build. Mater., Vol.16, pp.473-487, 2002.

[3] Thermoplastic Rubber/Bitumen Blends for Roof and Road, Bull A.L., and Vonk W.C., Shell Chemical Technical Manual, TR 8, p.15, 1984.

[4] Vyosokomol Soed I.A. Uskev:, 2, pp.926-930, 1960.

[5] Chemistry of Materials R.A. Vaia, H. Ishi, E.P. Giannelis:, 5-12, pp.1694-1696, 1993.

[6] Polymers, S.S. Ray, K. Okamoto: Prog. In Polym. Sci. 28-11, pp.1539-1641, 2003.

[7] Jr. M.E. Clarance, L.G. Martin, W.E. Chester, P.G. Dennis: U.S. Pat. No. 5.652.284. pp.1-6, 1977.

[8] Effect of Nano Clay Modification on the Rheology of Bitumen and on Performance of Asphalt Mixture, D.B. Ghile:. Ph D Thesis, Delft University of Technology, Netherlands, pp.1-151, 2006.

[9] Nanocomposite Polymers, M.S. Sureshkumar, D. Biondi, S. Fillipi, G. Polacco: Proc. Int. Conf. on Nanotechnology and Advanced Materials (ICNAM), University of Bahrain, Bahrain, p.138, 2009.

[10] Additives in Asphalt, King, G., Journal of Association of Asphalt Paving Technologists, No.68, pp.32–69, 1999.

[11] Styrene–Butadiene Rubber Latex Modified Asphalt, Bates, R. and Worch, R., Engineering Brief, No. 39, Federal Aviation Administration, Washington DC, 1987.

[12] Image Processing Dealing with Texture, Petrou, M., and Sevilla , P.G., Wiley, 2006.

[13] Texture Analysis of Polymer Modified Bitumen Images, Gümüştekin, Ş., Topal, A., Şengöz, B. International Journal of Materials Research, Vol.102, 513-520, 2011.
[14] Asphalt Modified by SBS Triblock Copolymer- Morphology and Model Chen, J., Liao, M., and Shiah, M., J. Mater Civil Eng., Vol.14 (3), pp.224–229, 2002.
[15] Paving Asphalt Polymer Blends, Relationship Between Composition, Structure and Properties, Brule, B., Brion, Y., and Tanguy, B., J. Assoc. Asphalt Paving Tech., Vol.57, pp.41–64, 1988.
[16] Rheological Evaluation of EVA Polymer Modified Bitumens, Airey, G. D., J. Constr. Build. Mater., Vol.16, pp.473–487, 2002.
[17] Sampling for Microscopy—Test Procedure, Wegan, V., "Danish Road Institute, 1996.
[18] Theory of Communications, Gabor, D., J. Inst. Elec.Eng., Vol.93, pp.429-457, 1946.
[19] Texture Features for Browsing and Retrieval of Image Data, Manjunath, B.S., and Ma, W.Y. IEEE Trans. On Pattern Analysis and Machine Intelligence, Vol.18, No.8, pp.837-842, 1996.
[20] Rotation-Invariant and Scale-Invariant Gabor Features for Texture Image Retrieval, Han, J., and Ma, K.K., Vol.25, Issue 9, pp.1474-1481, 2007.
[21] A Modified Gabor Function for Content Based Image Retrieval, Sastry, C.S., Ravindranath, M., Pujari, A.K., and Deekshatulu, B.L., Pattern Recognition Letters, Vol.28, Issue 2, pp.293-300, 2007.
[22] Image Retrieval via Isotropic and Anisotropic Mappings, Iqbal, Q., and Aggarwal, J.K., Pattern Recognition, Vol.35, Issue 12, pp.2673-2686, 2002.
[23] Efficient Texture Analysis of SAR Imagery, Kandaswamy, U., Adjeroh, D.A., and Lee, M.C., IEEE Trans. on Geoscience and Remote Sensing, Vol.43, Issue 9, pp.2075-2083, 2005.
[24] Segmentation of Gabor-filtered Textures Using Deterministic Relaxation, Raghu, P.P., and Yegnanarayana, B., IEEE Transactions on Image Processing, Vol.5, Issue 12, pp.1625-1636, 1996.
[25] An Automated Inspection System for Textile Fabrics Based on Gabor Filters, Mak, K.L., and Peng, P., Robotics and Computer-Integrated Manufacturing, Vol. 24, Issue 3, pp.359-369, 2008.
[26] Defect Detection in Textured Materials Using Gabor Filters, Kumar, A., and Pang, G.K.H., IEEE Transactions on Industry Applications, Vol.38, Issue 2, pp.425-440, 2002.
[27] Online Palmprint Identification, Zhang, D., Kong, W.K., You, J., and Wong, M., IEEE Trans. On Pattern Analysis and Machine Intelligence, Vol.25, Issue 9, pp.1041-1050, 2003.
[28] Palmprint Feature Extraction using 2-D Gabor Filters, Kong, W.K., Zhang, D., and Li, W., Pattern Recognition, Vol.36, Issue 10, pp.2339-2347, 2003.
[29] On Generation and Analysis of Synthetic Iris Images, Zuo, J., Schmid, N.A., and Chen, X., IEEE Trans. on Information Forensics and Security, Vol.2, Issue 1, pp.77 – 90, 2007.
[30] A Methodology for Identification of Fingerprints Based on Gabor Filter, Oliveira, S.L.G.D. and Assis, J.T.D., IEEE Latin America Transactions (Revista IEEE America Latina), Vol.4, Issue 1, pp.1-6, 2006.
[31] Fingerprint Matching from Minutiae Texture Maps, Benhammadi, F., Amirouche, M.N., Hentous, H., Beghdad, K.B., and Aissani, M., Pattern Recognition, Vol.40, Issue 1, pp.189-197, 2007.
[32] A Hybrid Fingerprint Matcher , Ross, A., Jain, A., Reisman, J., Pattern Recognition, Vol.36, Issue 7, pp.1661-1673, 2003.
[33] Gabor Feature Based Classification Using the Enhanced Fisher Linear Discriminant Model for Face Recognition, Liu, C., and Wechsler, H., IEEE Trans. Image Process., Vol.11, Issue 4, pp.467-476, 2004.
[34] Segmentation of Kidney from Ultrasound Images Based on Texture and Shape Priors, Xie, J., Jiang, Y., Tsui, H.T., IEEE Transactions on Medical Imaging, Vol.24, Issue 1, pp.45-57, 2005.
[35] Deformable Segmentation of 3-D Ultrasound Prostate Images Using Statistical Texture Matching Method, Zhan, Y., and Shen, D., IEEE Trans. on Medical Imaging, Vol.25, Issue 3, pp.256-272, 2006.
[36] Object Detection Using Gabor Filters, Jain, A.K., Ratha, N.K., and Lakshmanan, S.,Pattern Recognition, Vol.30, Issue 2, pp.295-309, 1997.
[37] Gabor Wavelet Representation for 3-D Object Recognition, Wu, X. and Bhanu, B., IEEE Trans. on Image Processing, Vol.6, Issue 1, pp.47-64, 1997.
[38] Text Analysis Using Local Energy, Chan, W. and Coghill, G., Pattern Recognition, Vol.34, Issue 12, pp.2523-2532, 2001.
[39] Personal Identification Based on Handwriting, Said, H.E.S., Tan, T.N., and Baker, K.D., Pattern Recognition, Vol.33, Issue 1, pp.149-160, 2000.
[40] Rotation Invariant Texture Features and Their Use in Automatic Script Identification Tan, T.N., IEEE Transactions on Pattern Analysis and Machine Intelligence, Vol.20, Issue 7, pp.751-756, 1998.
[41] Texture Classification Using Gabor Wavelets Based Rotation Invariant Features, Arivazhagan, S., Ganesan, L., and Priyal, S.P., Pattern Recognition Letters, Vol.27, pp.1976-1982, 2007.
[42] Invariance Properties of Gabor Filter Based Features, Overview and Applications, Kamarainen, J.K., Kyrki, V., and Kalviainen, H., IEEE Trans. on Image Processing, Vol.15, Issue 5, pp.1088-1099, 2006.
[43] Rotation-Invariant and Scale-Invariant Gabor Features for Texture Image Retrieval Han, J., and Ma, K.K., Image and Vision Computing, Vol.25, Issue 9, pp. 1474-1481, 2007.
[44] Rotation-Invariant Texture Classification, Lahajnar F., and Kovacic, S., Pattern Recognition Letters, Vol.24, Issues 9-10, pp.1151-1161, 2003.

[45] Rotation-Invariant Texture Classification Using a Complete Space-Frequency Model, Haley, G.M., and Manjunath, B.S., IEEE Trans. on Image Processing, Vol.8, Issue 2, pp.255-269, 1999.
[46] Robust Rotation-Invariant Texture Classification: Wavelet, Gabor Filter and GMRF Based Schemes Porter, R., and Canagarajah, N., Vision, Image and Signal Processing, IEE Proceedings- Vol.144, Issue 3, pp.180-188, 1997.
[47] Nearest Neighbor Pattern Classification, Cover, T.M. and Hart, P.E., IEEE Transactions on Information Theory, Vol. IT-13, pp. 21-27, 1967.
[48] Dimensionality Reduction: A Comparative Review, Van der Maaten, L.J.P., Postma, E.O., and Van den Herik, H.J. Tilburg University Technical Report, TICC-TR 2009-005, 2009.